Department of Biomedical Sciences

University of Veterinary Medicine Vienna

Institute of Animal Breeding and Genetics

Head: O.Univ.-Prof. Dr.med.vet. Mathias Müller

# Antiviral Properties of Carbon-Based Quantum Dots

Bachelor's Thesis

University of Veterinary Medicine Vienna

Submitted by

Melissa Satzinger

Vienna (July, 2023)

**Supervisors:**

Internal: Dr Tanja Bulat and Dr Birgit Strobl

External: Dr Danica Zmejkoski

# Acknowledgements

First and foremost, I would like to express my gratitude to my supervisors, Dr. Tanja Bulat, Dr. Danica Zmejkoski, and Dr. Birgit Strobl, for taking time out of their busy schedules to review my thesis and provide valuable feedback. A special thank you to Tanja for accepting me as an intern during my first semester at university already, and subsequently taking me back again in my fifth. Thank you for the countless opportunities to learn something new, and helping me every step along the way.

I also want to express my deepest gratitude to Dr. Danica Zmejkoski and the research team at the Institute of Nuclear Sciences “Vinča”, Dr. Zoran Marković and Biljana Todorović-Marković for letting me take part in this project and for synthesizing and providing the Carbon Quantum Dots used in my experiments. Thank you for giving me the opportunity to be part of something bigger than I ever would have expected as a bachelor’s student.

I would also like to thank Univ.-Prof. Dr. Mathias Müller, for allowing me to compose my thesis at his institute. Thank you to all the employees at the lab and the master’s and PhD students for being incredibly helpful and kind when it came to answering any questions I had, and for making me feel welcome from day one.

Finally, a big thank you to my boyfriend for the moral support, and to my parents for their patience and understanding as I slowly made my way here.

# Table of Contents

# 1 Introduction

## 1.1 Carbon quantum dots

Carbon quantum dots (CQDs) are small carbon nanoparticles of less than 10 nm in diameter and an average height of about 1–2 nm. CDQs have become of interest in many fields, such as bioimaging, drug delivery and nanomedicine [1]. They are valued for their low toxicity, good biocompatibility, high water solubility, chemical stability, and photoluminescence [2]. The morphology of CQDs encompasses two main forms: (i) disk-shaped with 1-3 layers of 2D graphene-like sheets with surface groups (honeycomb network) (Figure 1A) and (ii) a quasi-spherical network of carbon with various tuneable surface groups (Figure 1B). CQDs are sometimes also referred to as carbon dots (CDs) or carbon nanodots (CNDs) [3].

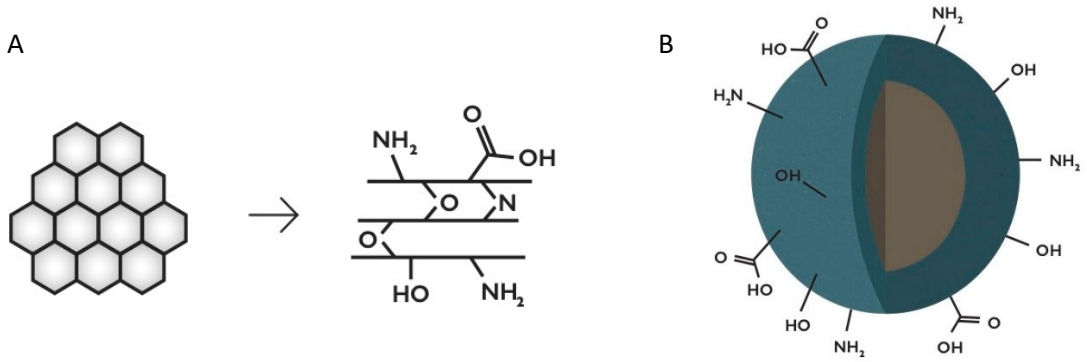


***Figure 1:*** *The two main morphologies of CQDs. A) Carbon dot disk structure; B) Carbon dot quasi-spherical structure (Modified from [3])*

CQDs were first discovered during the purification of single-walled carbon nanotubes by Xu et al. in 2004 [4]. Since then, many synthesis methods have been developed, which can generally be categorized into two groups: top-down synthesis and bottom-up synthesis (Figure 2) [1,5].

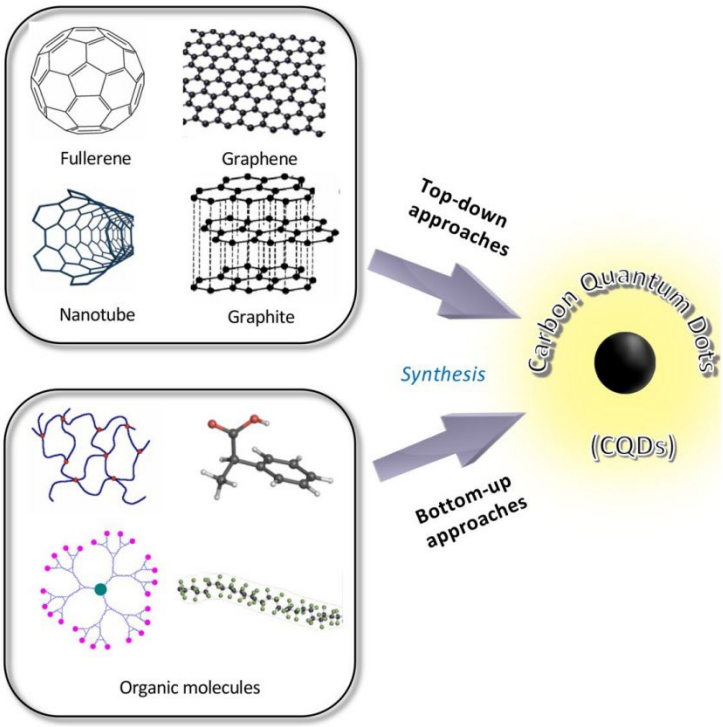


***Figure 2:*** *Top-down and bottom-up synthesis approaches of CQDs* [5]

Top-down synthesis includes breaking down larger carbon structures (graphite or activated carbon) using methods such as chemical and laser ablation, electrochemical carbonization and ultrasonic treatment. These methods usually involve high acidity, high potential, and high energy [1,5]. Bottom-up synthesis involves the formation of CQDs from molecular precursors, such as citrate or carbohydrates, and is more cost-effective, environmentally friendly and less time-consuming than top-down synthesis. The bottom-up synthesis methods include microwave-assisted, template, hydrothermal and thermal methods [6]. In the case of hydrothermal carbonization, a solution of the organic precursor is sealed and heated in a reaction vessel which will withstand the necessary temperatures for carbonization (up to 300°C) and keep the vapours in. The resulting high pressure improves the efficiency of the reaction. Possible precursors include glucose, citric acid, proteins, and juices such as bananas, oranges and strawberries [1,3,7]. Photoluminescent properties, surface functional groups, structure and composition vary depending on the precursor used and the reaction atmosphere, time and temperature [3,6]. Thermal decomposition involves the carbonization or pyrolysis of the large-sized carbonaceous precursors under higher temperatures, leading to easy

mass production of CQDs. Moreover, this method allows fine-tuning of fluorescent properties of CQDs by controlling reaction-mix pH, reflux duration, and reaction temperatures [6,8].

Several methods can be used to obtain purified CQDs with specific properties from the solution: filtration, centrifugation, dialysis, and column chromatography. Typically, the CQDs are contained in the supernatant after centrifugation, while the precipitant contains larger particles. In the case of dialysis, multiple membranes of different pore sizes can be used to select a specific size range of CQDs. While column chromatography is a relatively time-consuming method, it allows the selection of CQDs with more specific properties, such as polarity [3].

Surface functionalization can be used to tune CQDs' properties further. Surface functionalization impacts the capability of CQDs to interact with other organic molecules, drugs, and procaryotic and eucaryotic cells. Therefore, it can significantly alter cellular uptake, antibacterial activity and cytotoxicity of CQDs. Functionalization includes covalent bonding using surface amines or carboxylates, $\pi$-$\pi$ interactions and sol-gel technology. Doping with various elements, such as sulfur, phosphorus, and particularly nitrogen, by introducing additional components during synthesis changes the electronic structure and therefore leads to shifts in the CQDs' photoluminescent emission [7,9]. Besides surface functionalization, surface passivation can be used to increase the fluorescence intensities and shield CQDs from contaminants in their environment which could otherwise affect their properties [9].

CQDs find many applications in bioimaging and optical and electrochemical biosensing [1]. They are also used in photodynamic therapy for the treatment of tumours. Photosensitive molecules must be delivered into the tumour tissue, which then gets irradiated with a specific wavelength of light. This triggers the formation of reactive oxygen species (ROS), which subsequently causes cell death by inducing cleavage of DNA of the cancer cells [3]. The generation of ROS also allows CQDs to act as antibacterial agents [9]. Some CQDs have the ability to prevent or inhibit viral infections, depending on their surface chemical structure, composition, size and shape [5,10]. Du et al. studied the effect of CQDs on the replication of pseudorabies virus (PRV) and porcine reproductive and respiratory syndrome virus (PRRSV). They discovered that CQDs induce interferon-α (IFN-α) production and upregulate expression of IFN-stimulating genes (ISGs)[11].

Garg et al. report the antiviral activity of CQDs doped with triazole functionalized heteroatom co-doped CQDs (TFH-CQDs) against human coronavirus [12].

## 1.2 Cytomegalovirus

Cytomegalovirus (CMV), a genus of viruses in the family of *Herpesviridae*. As all herpesviruses, CMV has a double-stranded DNA genome. The virus capsid is surrounded by the tegument, a cluster of proteins, and enveloped by a lipid bilayer membrane that contains glycoproteins necessary for attachment to and subsequent infection of the host cell (Figure 3). Once internalized, the virus particle is dismantled, and the genome enters the host cell's nucleus, where it is replicated and transcribed to mRNA. After primary infection, virus persists in the organism for a lifetime and is able to reactivate when the immune system becomes compromised [13].

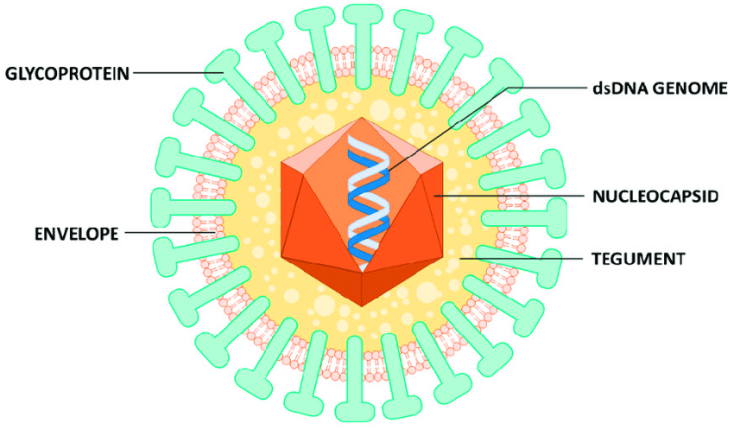


***Figure 3:*** *Structure of CMV* [14]

CMV is species-specific. Human cytomegalovirus (HCMV), also known as human beta herpesvirus 5 (HHV-5), infection is very common across the globe. The proportion of adults with specific IgG antibodies is ~60% in developed countries and ~90% in developing countries [13]. In immunocompromised individuals (e.g. elderly and transplantation patients), HCMV infection can lead to inflammation of the lungs or brain, bone marrow failure, and organ failure [15]. The virus can be transmitted from mother to foetus, where newborns risk developing mental retardation, deafness and microencephaly[16]. Although the development of a vaccine against HCMV has been underway

for years, none has yet been licensed due to low efficiency [17]. Emerging resistance to ganciclovir, an antiviral drug used for the treatment of CMV infections, underscores the pressing need for new antiviral treatment options [18,19].

## 1.3 Antiviral mechanism of cells

Interferons (IFNs) are the first line of defense against viral infection and a key component of the innate immune response. They are cytokines which are involved in pathways that lead to the degradation of viral RNA, blocking of viral transcription, and inhibition of translation. Three types of IFNs have been identified. Type I is comprised of IFNα, IFNβ, IFNκ, IFNε, IFNo, IFNτ and IFN$\delta$. Type II only contains IFNγ, and type III only contains IFNλ. The types are distinguished by which receptor complex they signal through (Figure 4). Type I uses IFNAR (interferon alpha/beta receptor), type II uses IFNGR (interferon gamma receptor), and type III uses IFNLR1 (interferon lambda receptor 1) as well as IL-10R2 (interleukin-10 receptor). Type I IFNs are known to be essential for a robust immune response against viral infection. IFNAR-deficient mice have increased susceptibility to viruses, but a regular resistance to other microbial pathogens. Humans with genetic defects in components in the IFNAR signaling pathway, such as STAT1 (signal transducer and activator of transcription 1), die of viral disease [20].

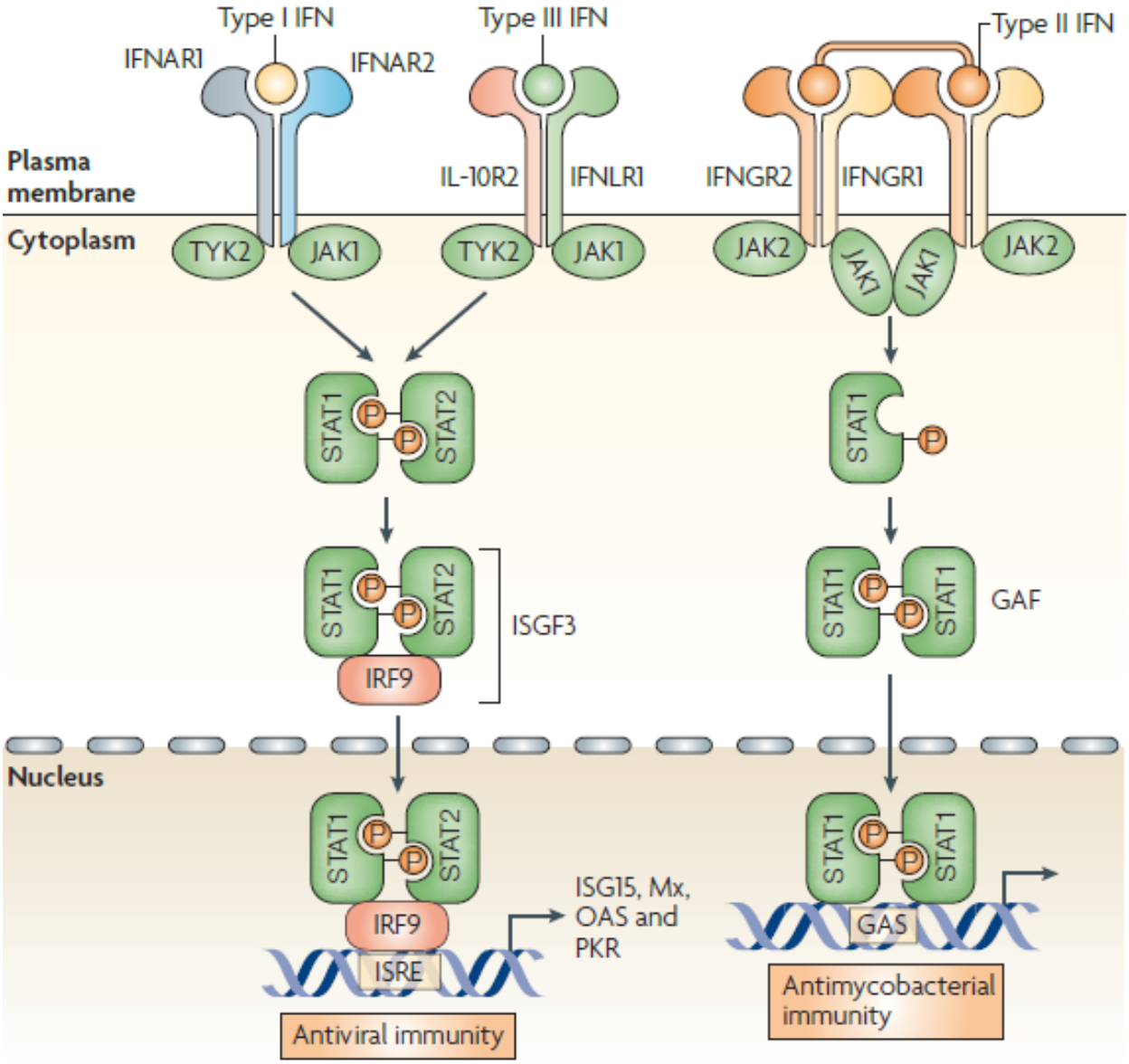


***Figure 4:*** *Interferon receptor signaling. The function of the IFNs is mediated through three receptor complexes: Type I IFNs bind to a heterodimer of IFNAR1 and IFNAR2; IFNλ binds to IFNLR1 in association with IL-10R2; and dimers of IFNγ are bound by a tetramer comprising two IFNGR2 chains and two IFNGR1 chains* [20].

The binding of IFN I to the IFNAR receptor complex initiates a signaling cascade which leads to the induction of more than 300 IFN-stimulated genes (ISGs). Many of these genes encode pattern-recognition receptors (PRRs) which detect viral molecules, or transcription factors which form an amplification loop resulting in more IFN production. Some ISGs also encode proteins

with potential for direct antiviral activity. These proteins include the Mx (myxovirus resistance) family, PKR (protein kinase R), RNaseL (ribonuclease L), and ISG15 (IFN-stimulated protein of 15kda). Mx proteins are induced by type I as well as type III IFNs. The protein family includes Mx1 and Mx2 in mice, and MxA and MxB in humans. Genetic studies of human populations have shown a correlation between a polymorphism in the *MXA* gene and the susceptibility of several viruses including hepatitis C and measles. PKR is expressed as an inactive kinase that gets activated by viral RNA and upregulated by type I IFNs. The active form of PKR leads to the halt of translation and allows the cell to reconfigure gene expression. It also induces cellular responses by modulating cell-signaling pathways. Experiments with PKR-deficient mouse embryonic fibroblasts have shown that PKR plays a role in protecting against infection with several RNA and DNA viruses. The RNaseL pathway is directed by OASL (2', 5'-oligoadenylate synthetase-like), which is expressed in low levels in unstimulated cells and considerably induced by type I IFNs. RNaseL can mediate RNA degradation, causing the activation of other cytoplasmic PRRs which lead to the induction of type I IFN gene expression. Cells deficient in RNaseL show decreased IFNβ expression due to the lack of signaling through these PRRs. Finally, ISG15 has been shown to prevent virus-mediated degradation of IRF3 (IFN-regulatory factor 3), leading to increased IFNβ expression [20].

# 2 Hypothesis and aims

This project is based on the hypothesis that a pre-treatment with CQDs leads to an improved cellular antiviral defence against CMV. The specific aims of this thesis were to (i) test antiviral properties of CQDs against CMV, using murine cytomegalovirus (MCMV) as a model virus, (ii) analyse effects of CQDs on the expression of ISGs and (ii) evaluate cytotoxicity of CQDs using cell proliferation and apoptosis assays in primary murine fibroblasts.

# 3 Material and Methods

## 3.1 Material

| ***Table 1:*** *Plastics* | | |
|---|---|---|
| **Name** | **Company** | **Product Number** |
| SafeSeal microtube 2 ml | Sarstedt | # 72.695.500 |
| SafeSeal microtube 1.5 ml | Sarstedt | # 72.690.001 |
| Tubes 50 ml | Greiner Bio-One | # 210261 |
| Tubes 15 ml | Sarstedt | # 62.554.502 |
| Cell strainers | Miltenyi | # 130-110-917 |
| Round bottom polystyrene tubes 5 ml | Falcon | # 352008 |
| PCR 8-tube strips 0.2 ml | Greiner Bio-One | # 673210 |
| Hard-Shell PCR plates 96 well | Bio-Rad | # HSP9601 |
| PCR plate seals | Bio-Rad | # MSB1001 |
| Tissue culture plates 6 well | Falcon | # 353224 |
| Tissue culture plates 24 well | Falcon | # 353226 |
| Tissue culture plates 96 well | Falcon | # 353075 |
| Tissue culture dishes | Sarstedt | # 83.3903 |

| ***Table 2:*** *Buffers and media* | | |
|---|---|---|
| **Name** | **Company** | **Product Number** |
| Dulbecco's Phosphate Buffered Saline | Sigma-Aldrich | # D8537 |
| RPMI-1640 Medium | Sigma-Aldrich | # R8758 |
| Fixation buffer | BioLegend | # 420801 |
| MACS buffer | Miltenyi | # 130-091-221 |

| ***Table 3:*** *Chemicals, reagents and commercial assays* | | |
|---|---|---|
| **Name** | **Company** | **Product Number** |
| Penicillin-Streptomycin | Sigma-Aldrich | # P0781 |
| FCS | Gibco | # 10270-098 |
| L-Glutamine | Sigma-Aldrich | # G7513 |
| ß-Mercaptoethanol | Sigma-Aldrich | # M3148 |
| Trypan blue | Sigma-Aldrich | # T8154 |
| TRIzol | Thermo Fisher | # 15596026 |
| Chloroform | Carl Roth | # 3313.2 |
| Isopropanol | Carl Roth | # 6752.2 |
| Ethanol | Scharlau | # ET00051000 |
| Nuclease-free water | Sigma-Aldrich | # W4502-1L |
| Glycogen | Sigma-Aldrich | # 10-901-393-001 |
| SuperScript IV First-Strand Synthesis System | Thermo Fisher Scientific | # 18091050 |
| Sulforhodamine B | Sigma-Aldrich | # 230162 |
| Acetic Acid | Carl Roth | # 3738.4 |
| TCA | Sigma-Aldrich | # T8657 |
| Tris base | Sigma-Aldrich | # 10708976001 |
| $MgCl_2$ 25 mM | Solis BiodDyne | # 05-11-00050 |
| dNTP mix, 100 mM | Thermo Fisher Scientific | # R0182 |
| 10 x Reaction buffer B | Solis BioDyne | # 01-02-01000 |
| HOT FIREPol DNA Polymerase | Solis BioDyne | # 01-02-01000 |

| ***Table 4:*** *Flow cytometry antibodies and dyes* | | | | |
|---|---|---|---|---|
| **Name** | **Fluorochrome** | **Clone** | **Company** | **Product Number** |

| | | | | |
|---|---|---|---|---|
| Annexin V | FITC | N/A | BD Biosciences | # 560931 |
| Fixable Viability Dye | APC-Cy7 | N/A | Thermo Fisher Scientific | # 65-0865-18 |

| ***Table 5:*** *Mice* | |
|---|---|
| **Organism/ Strain** | **Product Number** |
| C57BL/6N | N/A |

| ***Table 6:*** *qPCR primers, assays and dye* | | |
|---|---|---|
| **Name** | **Company** | **Product Number** |
| *Il1b* | Qiagen | # QT01048355 |
| *Irf7* | Qiagen | # QT00245266 |
| *Oas1a* | Qiagen | # QT01056048 |
| *Stat1* | Qiagen | # QT01149519 |
| *Stat2* | Qiagen | # QT00160216 |
| *Pkr*-fwd 5'-CAG TGT GAG CCC AAC TCT GA-3' | Sigma-Aldrich | N/A |
| *Pkr*-rev 5'-GCT GAC TGG GAA ACA CCA TT-3' | Sigma-Aldrich | N/A |
| *Mx1*-fwd 5'CCT GGA GGA GCA GAG TGA CAC-3' | Sigma-Aldrich | N/A |
| *Mx1*-rev 5'GGT TAA TCG GAG AAT TTG GCA-3' | Sigma-Aldrich | N/A |
| *Mx1*-probe 5'-TTA AGG CTG GAT GAG GCT CGG CAG A-3' | Sigma-Aldrich | N/A |
| *Tnfa*-fwd 5'-CAA AAT TCG AGT GAC AAG CCT G-3' | Sigma-Aldrich | N/A |

| | | |
|---|---|---|
| *Tnfa*-rev 5'-GAG ATC CAT GCC GTT GGC-3' | Sigma-Aldrich | N/A |
| *Tnfa*-probe 5'-AGC CCA CGT CGT AGC AAA CCA CC-3' | Sigma-Aldrich | N/A |
| *Ube2d2*-fwd 5'-AGG TCC TGT TGG AGA TGA TAT GTT-3' | Sigma-Aldrich | N/A |
| *Ube2d2*-rev 5'-TTG GGA AAT GAA TTG TCA AGA AA-3' | Sigma-Aldrich | N/A |
| *Ube2d2*-probe 5'-CCA AAT GAC AGC CCC TAT CAG GGT GG-3' | Sigma-Aldrich | N/A |
| Quantitect SYBR Green PCR Kit | Qiagen | # 204345 |
| EvaGreen Dye | Biotium | # 31000 |

***Table 7:*** *Software*

| **Name** | **Company** | **Product Number** |
|---|---|---|
| CytExpert | Beckman Coulter Life Sciences | N/A |
| GraphPad Prism 9 | GraphPad Software | N/A |
| FlowJo | BD Life Science | N/A |

## 3.2 Methods

### 3.2.1 Synthesis and characterization of CQDs

Synthesis of CQDs was done by our collaborators at the Institute of Nuclear Sciences „Vinča". CQDs were produced by pyrolysis from citric acid. CQDs were characterized by different techniques such as atomic force microscopy (AFM), Fourier transformed infrared spectroscopy (FTIR), and electron paramagnetic resonance (EPR). CDQs were dissolved in PBS for *in vitro* experiments.

### 3.2.2 Cells

We used C57BL/6N mice for producing primary mouse embryonic fibroblasts (pMEFs) according to the published protocol [21]. Heads and livers were removed from 13-14 days old mice embryos. The rest was minced with scissors and resuspended in PBS supplemented with penicillin (50 µg/mL)/streptomycin (50 U/mL) and filtered through a strainer (100 µm). Cells were pelleted down by centrifugation at 200 × *g* for 5 minutes. After washing cells two times with PBS, $5 \times 10^6$ cells were plated per 10 cm dish in complete medium containing DMEM (high glucose), 10% FCS (heat-activated), Penicillin/Streptomycin (100 µg/mL and 100 U/mL), 2mM L-glutamine and 50 µM beta-mercaptoethanol. The cells were divided and preserved in liquid nitrogen containing 10% DMSO in FCS upon reaching confluency. In all experiments, the pMEFs used were at a passage number lower than four and cultivated until sub-confluent. All animal experiments were performed by trained personnel, approved by the institutional ethics and animal welfare committee and the national authority according to §§ 26ff. of the Animal Experiments Act, Tierversuchsgesetz 2012 - TVG 2012 (BMWFW 68.205/0173-V/3b/2019) and conform to the guidelines of FELASA and ARRIVE.

### 3.2.3 Virus

Tissue culture-derived (TC) murine cytomegalovirus (MCMV) Smith strain (American Type Culture Collection, ATCC® VR194) was used.

### 3.2.4 CQDs treatment

For all experiments, pMEFs were seeded into tissue culture dishes or 6-, 24- or 96-well plates based on the assays. After seeding, cells were cultivated for 24 h in the medium. After verifying confluency under a microscope, the medium was replaced (i) with a new medium for control samples, (ii) with medium containing 1% PBS for PBS control, (iii) with medium including CQDs at concentrations of 0.05 mg/mL or 0.005 mg/mL. The cells were then incubated for 24 hours and prepared for downstream analysis.

### 3.2.5 Plaque assay

$1 \times 10^4$ cells/well in a 24-well plate were treated with CQDs or corresponding controls. Following the removal of the medium, cells were infected with TC-MCMV at three distinct concentrations ($2.38 \times 10^3$ PFU/ml, $2.38 \times 10^2$ PFU/ml, $0.238 \times 10^2$ PFU/ml) using centrifugation

enhancement (110 × *g* for 30 minutes at room temperature) followed by 90 minutes incubation at 37°C, 5% $CO_2$. After removing the virus inoculum, cells were overlaid with 1% low-melting agarose in growth medium. Three to four days post-infection, the MCMV plaques were counted under a microscope.

### 3.2.6 Flow cytometry

$1 \times 10^6$ pMEFs were seeded into tissue culture plates, treated with 0.05 mg/mL CQDs for 24 hours. Cells were exposed to 1% H2O2 for 3 hours to serve as a positive control for apoptosis. Subsequently, the cells were detached with a rubber scraper, and a single-cell suspension was achieved by resuspending with a 1 mL pipet. Cells were incubated with Viability staining (working dilution 1:1000) and Annexin-V (working dilution 1:100) in the dark for 20 minutes at 4°C. Cells were then washed with PBS and analysed using a CytoFlex flow cytometer.

### 3.2.7 Sulforhodamine B colorimetric assay

To determine the potential cytotoxic effect of CQDs on pMEFS, we used a Sulforhodamine B (SRB) colourimetric assay as previously described [22]. $2 \times 10^3$ cells were seeded into a 96-well plate and treated with CQDs for 24 hours. Treatment was removed and cells were in medium for additional 24 hours, 48 hours or 72 hours. Cells were fixed with ice cold 10% (wt/vol) trichloroacetic acid (TCA) for 1 hour at 4°C, rinsed with water, air-dried and stained with 0.057% (wt/vol) SRB solution in 1% acetic acid for 30 minutes at room temperature. Cells were washed with acetic acid to remove any unbound dye and again left to dry at room temperature. To each well, 10 mM Tris base solution was added and incubated on a gyratory shaker for 5 minutes to solubilize the dye. Subsequently, optical density (OD) was measured on a plate reader at 510 nm. The viability of untreated cells (control) was set to 100%, and the viability of treated cells was expressed as a percentage of the control.

### 3.2.8 RNA isolation and RT-qPCR

$5 \times 10^5$ pMEFs were seeded into 6-well plates and treated with two different concentrations of CQD (0.05 mg/mL or 0.005 mg/mL) or PBS control for 24 hours. Cells were harvested and total RNA was isolated using TRIzol. As a carrier, 0.5 µL of glycogen was added to each sample. The concentrations and quality of RNA was measured with a NanoDrop microvolume spectrophotometer. SuperScript™ IV First-Strand Synthesis System (Invitrogen) was used for

reverse transcription, following the manufacturer's protocol. The resulting samples were subsequently diluted 1:3 with nuclease-free water. Using the sample with the highest concentration (determined in the pre-run), standard curves were prepared using serial 4-fold dilutions. For each RT-qPCR, the threshold was set at the relative fluorescence (RFU) of 300 on a logarithmic scale. Quality controls were: $\Delta CT \leq 0.5$ for technical duplicates, $R2 \geq 0.99$ for standard curve and qPCR efficiencies (E) was $90\% \leqq E \geqq 105\%$. Gene expression was calculated relative to the housekeeping gene (HKG) *Ube2d2*.

### 3.2.9 Statistic analysis

Statistical analysis was performed in GraphPad Prism 9, using Student's t-test. Differences were interpreted as significant if a p-value $\leq 0.05$ was reached (* $p < 0.05$; ** $p < 0.01$; *** $p < 0.001$; **** $p < 0.0001$). p-values between 0.05 and 0.1 are indicated in graphs.

# 4 Results

## 4.1 CQDs are highly biocompatible

CQDs cytotoxicity on pMEFs was determined via SRB assay for proliferation and Annexin V flow cytometric analysis for apoptosis (Figure 5A). Exposure to CQDs (0.05 mg/mL) did not affect cell proliferation 48 or 72 hours after treatment, as demonstrated in Figure 5B. Although slightly higher cell proliferation was visible 24 hours following treatment, it did not attain the predetermined threshold for statistical significance *($p<0.05$)*. Subsequently, apoptosis analysis was performed 24 hours after CQD treatment. The viability of CDQs treated cells was comparable with viability of control cells as shown in Figure 5C. Furthermore, no significant variations were found in the frequency of early and late apoptotic cells between the CQD-treated and control samples (Figure 5C). In summary, our findings suggest that CQDs exhibit excellent biocompatibility with pMEFs.

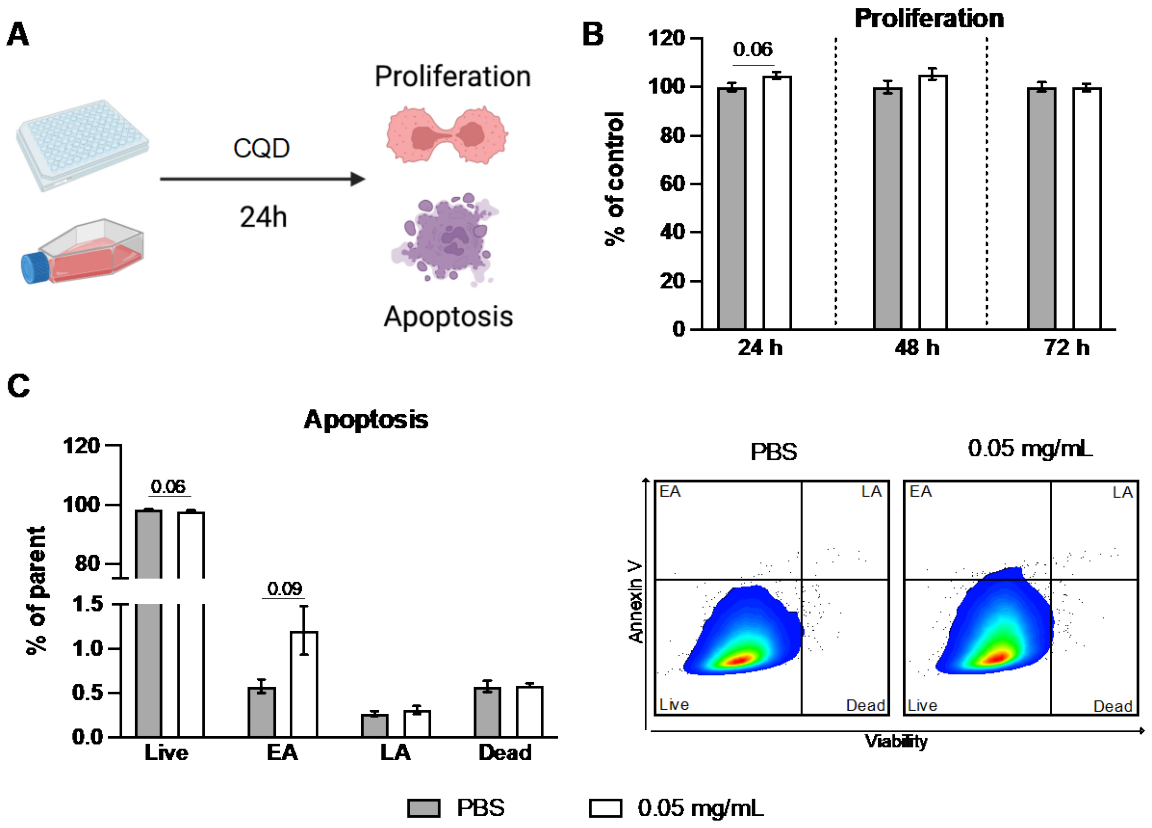


***Figure 5:*** *Biocompatibility assessments of CQDs. (A) Experimental design. (B) The proliferation of the cells was measured at different time points after CQDs treatment. (C) Apoptosis analysis with representative flow cytometry plots 24 hours after CQDs administration. EA – early apoptosis, LA – late apoptosis. Mean ± SEM are given. For all experiments n=4, N=2; n – biological replicates, N – experimental repetitions.*

## 4.2 Pre-treatment with CQDs reduces viral plaque formation

The antiviral efficacy of CQDs against MCMV was evaluated using a plaque-forming unit (PFU) assay, as depicted in Figure 6A. The PFU assay is a well-established method for measuring virus concentrations. The number of plaques relates to the infectious dose and the ability of viruses to infect cells through subsequent infection cycles. Permissive cells are infected with TC-MCMV. A Semisolid overlay is applied over the cells to limit the transmission of the infection to adjacent cells. A significant decrease of PFUs could be seen in the 0.05 mg/mL samples compared to control samples (Figure 6B). This data suggests that treatment with CQDs leads to a lower viral spread, and that this effect is dose-dependent.

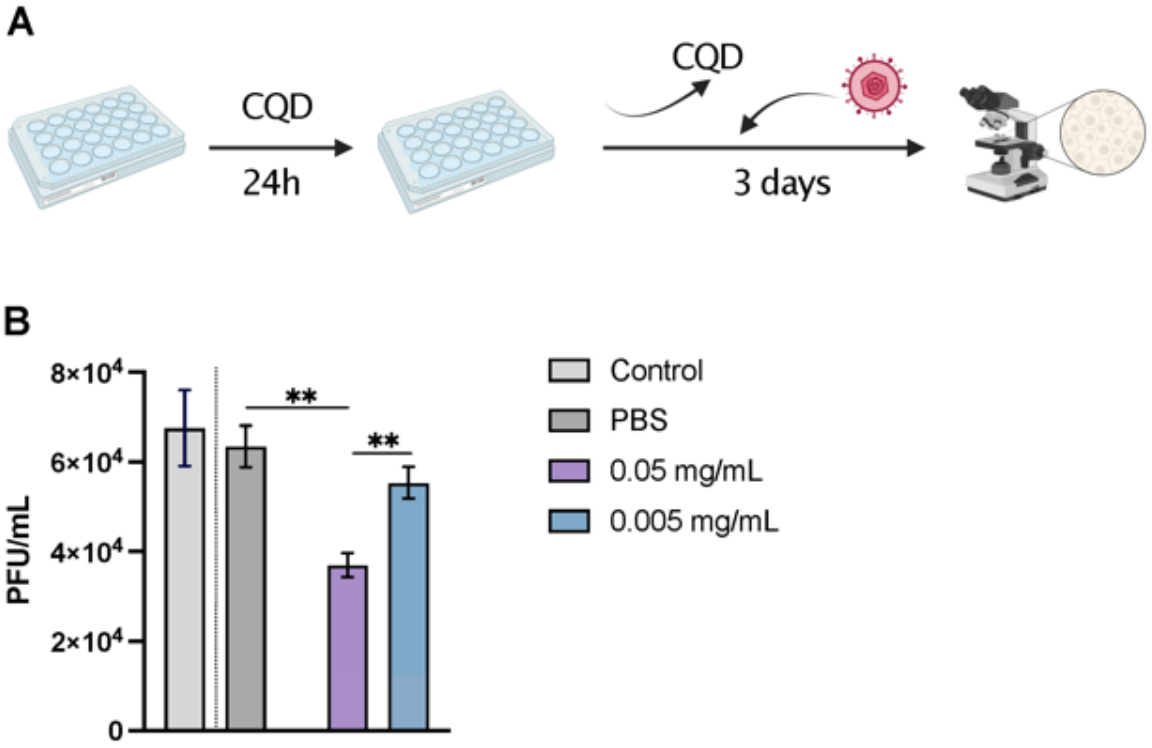


***Figure 6:*** *Assessment of the antiviral potential of CQDs against MCMV. (A) Experimental design. (B) Viral titers of control, PBS control, and CQD-treated cells. Mean ± SEM are given. **p ≤ 0.001. n=4, N=2; n-biological replicates, N-experimental repetitions.*

## 4.3 Pre-treatment with CQDs upregulates ISGs

In order to further explore the antiviral mechanism of CQDs, the expression of several genes involved in the cellular antiviral defense was analyzed using RT-qPCR from CQD-treated pMEFs (Figure 7A). IFNs have a significant role in the restriction of viral replication in host cells by upregulating the expression of ISGs, many of which encode proteins with antiviral effector functions [23]. mRNA expression of *Stat1, Stat2, Mx1*, *Irf7*, *Oas1* and *Pkr,* all of which are well-known ISGs, was notably increased in response to CQD treatment in a dose-dependent manner (Figure 7B). Tumour necrosis factor alpha (TNF-α) and interleukin-1beta (IL-1β) are cytokines that promote inflammation and are capable of aiding in virus control [24,25]. As shown in Figure 7B, treatment with CQDs led to significant upregulation of mRNA expression for both *Tnfa* and *Il-1b*. These results suggest that CQD treatment induces the upregulation of ISGs and pro-inflammatory cytokines.

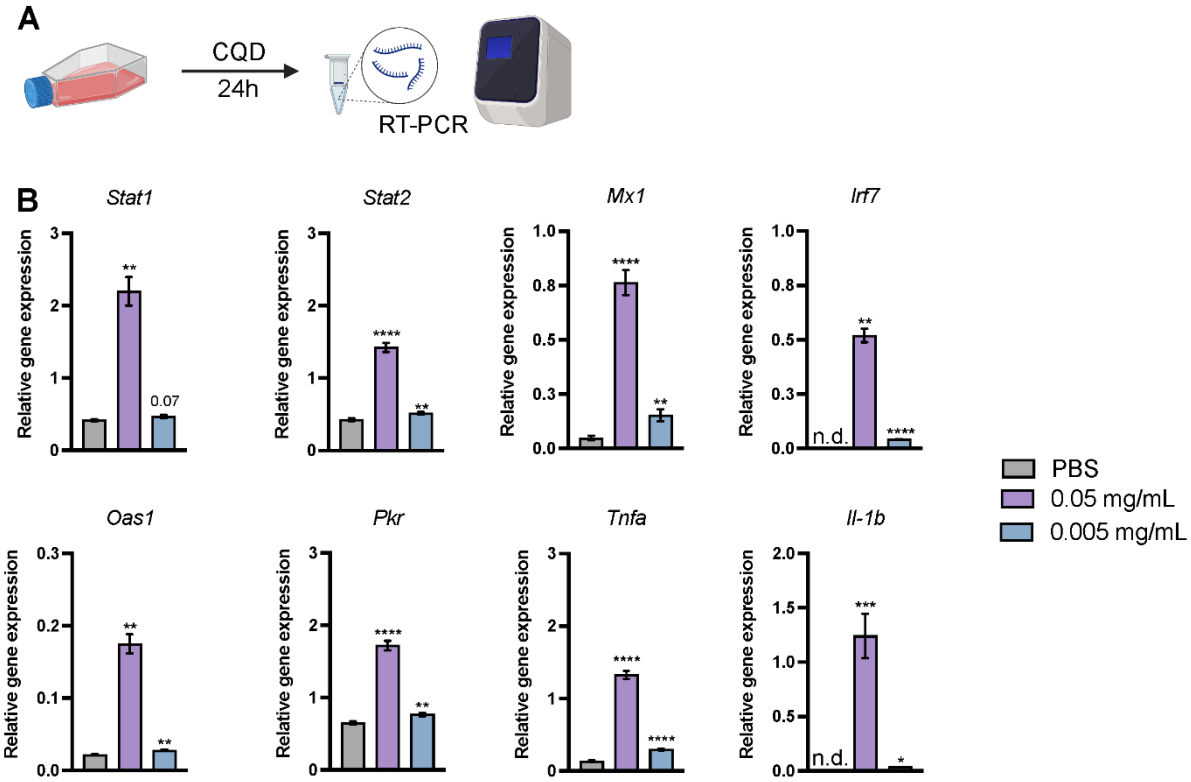


***Figure 7:*** *Effect of CQDs on the expression of ISGs, Tnfa and Il-1b. (A) Experimental design. (B) Relative gene expression. Mean ± SEM are given. Compared to PBS: *p ≤ 0.05, **p ≤ 0.01, ***p ≤ 0.001, **p ≤ 0.0001. n=4-6, N=2; n-biological replicates, N-experimental repetitions. n.d. – not detectable.*

# 5 Discussion

In this study, we analyse the cytotoxicity of CQDs produced by pyrolysis from citric acid in pMEFs and test their antiviral potency against MCMV. We were able to show that CQDs made in this way have low cytotoxicity and a dose-dependent antiviral activity against MCMV.

We show that pre-treatment of pMEFs with CQDs leads to a strong upregulation of ISGs. However, the exact mechanism behind this is unknown. Du et al. show that carbon dots produced by PEG-diamine and ascorbic acid induce interferon-α (IFNα) production. IFNα acts autocrine and paracrine and leads to the upregulation of ISGs and a better defence against virus infection, including PRV and PRRSV [11]. There is evidence that even without IFN receptors, ISGs can be upregulated [26]. Interferon regulatory factor 1 (IRF1) and interferon regulatory factor 3 (IRF3) are central regulators of IFN-independent ISGs expression [27]. Ag2S nanocrystals, a different kind of nanoparticle, have been shown to promote the production of IRF3 in a study on human coronavirus [28]. Through which mechanism citric acid-based CQDs induce upregulation of ISGs needs to be addressed in future research. Even though we were focused on ISGs in our studies, we cannot exclude other antiviral mechanisms. For example, Barras et al. show that carbon nanodots (C-dots) surface-functionalized with a boronic acid or amine functions block herpes simplex virus type 1 (HSV-1) interaction with the host cells and therefore repress virus invasion [29]. To investigate this possibility, cell morphology can be examined under an electron microscope to determine whether virus invasion has occurred. Additionally, the virions can be examined using transmission electron microscopy to visualize the virus-CQD interaction. Furthermore, we only researched the effect of CQDs on a genetic level, so Western blot analysis could be used to investigate the levels of viral proteins in treated and untreated samples for further insight.

Various metals, metal oxide and hybrid nanoparticles have been employed as antiviral agents in the past. Nevertheless, cytotoxicity, cost-effectiveness and ease of synthesis are multiple challenges [5,9]. The CQDs used in this study were synthesized from citric acid via pyrolysis, a comparatively simple and low-cost method. Paired with their excellent biocompatibility, this makes CQDs a very promising potential antiviral agent against CMV.

# 6 Summary

Carbon quantum dots (CQDs) are small, carbon-based nanoparticles, valued for their excellent biocompatibility, chemical stability, and strong photoluminescence, with antibacterial, anticancer, and antiviral properties. CQDs can be easily synthesized via top-down (breaking down larger carbon structures, such as graphite) or bottom-up (formation from molecular precursors, such as citrate) methods. CQDs used in this study were synthesized via a bottom-up approach from citric acid.

We performed cytotoxicity assays on these CQDs using (i) Sulforhodamine B (SRB) assay to examine effects on cell proliferation, and (ii) Annexin V flow cytometric analysis to examine the induction of apoptosis in primary mouse embryonic fibroblasts (pMEFs). Our results indicate a high biocompatibility of CQDs. Next, we investigated the antiviral properties of CQDs against murine cytomegalovirus (MCMV) using a plaque-forming unit (PFU) assay. Cells were pre-treated with CQDs (0.05 mg/mL and 0.005 mg/mL) for 24 hours and subsequently infected with MCMV. Viral plaques were counted under a microscope, and a significant decrease could be observed in CQD-treated samples in a dose-dependent manner. To better understand the antiviral effect, we isolated RNA from CQD-treated and untreated pMEFs. We performed RT-qPCR to quantify the expression of ISGs (e.g. *Stat1, Stat2, Irf7, Prk* etc.), *Tnfa* and *Il-1b*, which all are genes encoding proteins that are involved in the antiviral defence. All tested genes were upregulated in CQDs-treated samples in a dose-dependent manner. Our data indicate that CQDs produced from citric acid might be promising candidates for creating novel antiviral agents against CMV.

# 7 Zusammenfassung

Carbon quantum dots (CQDs) sind kleine, auf Kohlenstoff basierende Nanopartikel, die für ihre hervorragende Biokompatibilität, chemische Stabilität und starke Photolumineszenz geschätzt werden. Des weiteren besitzen sie antibakterielle, krebshemmende und antivirale Eigenschaften. CQDs können leicht durch „Top-Down-“ (Abbau größerer Kohlenstoffstrukturen, wie z. B. Graphit) oder „Bottom-Up“-Methoden (Bildung aus molekularen Vorläufern, wie z. B. Citrat) synthetisiert werden. Die in dieser Studie verwendeten CQDs wurden über einen Bottom-up-Ansatz aus Zitronensäure synthetisiert.

Wir analysierten die Zytotoxizität dieser CQDs auf primäre murine Fibroblasten (pMEFs) mittels (i) Sulforhodamin B- (SRB-) Tests zur Untersuchung der Auswirkungen auf die Zellproliferation und (ii) Annexin V-Durchflusszytometrie zur Untersuchung der Induktion von Apoptose. Unsere Ergebnisse weisen auf eine hohe Biokompatibilität der CQDs hin. Als Nächstes untersuchten wir die antiviralen Eigenschaften von CQDs gegen das murine Cytomegalovirus (MCMV) mit Hilfe eines PFU-Assays (Bestimmung von Plaque-bildenden Einheiten). Die Zellen wurden 24 Stunden mit CQDs (0.05 mg/mL und 0.005 mg/mL) behandelt und anschließend mit MCMV infiziert. Die viralen Plaques wurden unter dem Mikroskop gezählt. Wir konnten in den mit CQD behandelten Zellen einen dosisabhängigen, signifikanten Rückgang der Anzahl viraler Plaques nachweisen. Um die antivirale Wirkung besser zu verstehen, isolierten wir RNA aus CQD-behandelten und unbehandelten pMEFs und quantifizierten die Expression von ausgewählten ISGs (z. B. *Stat1, Stat2, Irf7* und *Prk*), *Tnfa* und *Il-1b* mittels RT-qPCR. Diese Gene kodieren alle für Proteine, die an der antiviralen Abwehr beteiligt sind. Wir konnten zeigen, dass alle getesteten Gene durch CQD-Behandlung dosisabhängig hochreguliert werden. Unsere Daten deuten darauf hin, dass aus Zitronensäure hergestellte CQDs vielversprechende Kandidaten für die Entwicklung neuer antiviraler Mittel gegen CMV sein könnten.

## Abbreviations

CQD, carbon quantum dots

CDs, carbon dots

CMV, cytomegalovirus

CNDs carbon nanodots

CQDs, carbon quantum dots

DMEM, Dulbecco's modified eagle medium

DMSO, dimethyl sulfoxide

FCS, fetal calf serum

HCMV, human cytomegalovirus

HIV, human immunodeficiency virus

HSV-1, herpes simplex virus 1

IFNs, interferons

IFNAR, interferon alpha/beta receptor

IFNGR, interferon gamma receptor

IFNLR1, interferon lambda receptor 1

IL, interleukin

IL-10R2, interleukin-10 receptor

IRF, interferon-regulatory factor

ISGs, interferon-stimulated genes

ISG15, IFN-stimulated protein of 15kda

MCMV, murine cytomegalovirus

Mx, myxovirus resistance

OASL, 2', 5'-oligoadenylate synthetase-like

PBS, phosphate buffered saline

PEDV, porcine epidemic diarrhea virus

PEG, polyethylene glycol

PFU, plaque-forming unit

PKR, protein kinase R

pMEFs, primary mouse embryonic fibroblasts

PRR, pattern-recognition receptor

qPCR, quantitative polymerase chain reaction

RNaseL, ribonuclease L

ROS, reactive oxygen specie

RT, reverse transcription

SRB, Sulforhodamine B

STAT1, signal transducer and activator of transcription 1

TC, tissue culture

TCA, trichloracetic acid

TNF, tumor necrosis factor

UBE2D2, ubiquitin conjugating enzyme E2 D2

# Tables and Figures

## Tables



## Figures

# References


1 Namdari, P., Negahdari, B. & Eatemadi, A. Synthesis, properties and biomedical applications of carbon-based quantum dots: An updated review. *Biomed Pharmacother* **87**, 209-222, doi:10.1016/j.biopha.2016.12.108 (2017).

2 Molaei, M. J. Carbon quantum dots and their biomedical and therapeutic applications: a review. *Rsc Adv* **9**, 6460-6481, doi:10.1039/c8ra08088g (2019).

3 Jorns, M. & Pappas, D. A Review of Fluorescent Carbon Dots, Their Synthesis, Physical and Chemical Characteristics, and Applications. *Nanomaterials-Basel* **11**, doi:ARTN 1448 10.3390/nano11061448 (2021).

4 Xu, X. *et al.* Electrophoretic analysis and purification of fluorescent single-walled carbon nanotube fragments. *J Am Chem Soc* **126**, 12736-12737, doi:10.1021/ja040082h (2004).

5 Xue, Y. X., Liu, C. C., Andrews, G., Wang, J. Y. & Ge, Y. Recent advances in carbon quantum dots for virus detection, as well as inhibition and treatment of viral infection. *Nano Converg* **9**, doi:ARTN 15 10.1186/s40580-022-00307-9 (2022).

6 Mansuriya, B. D. & Altintas, Z. Carbon Dots: Classification, Properties, Synthesis, Characterization, and Applications in Health Care-An Updated Review (2018-2021). *Nanomaterials (Basel)* **11**, doi:10.3390/nano11102525 (2021).

7 Arcudi, F., Dordevic, L. & Prato, M. Design, Synthesis, and Functionalization Strategies of Tailored Carbon Nanodots. *Acc Chem Res* **52**, 2070-2079, doi:10.1021/acs.accounts.9b00249 (2019).

8 Tajik, S. *et al.* Carbon and graphene quantum dots: a review on syntheses, characterization, biological and sensing applications for neurotransmitter determination. *Rsc Adv* **10**, 15406-15429, doi:10.1039/d0ra00799d (2020).

9 Wang, Y. F. & Hu, A. G. Carbon quantum dots: synthesis, properties and applications. *J Mater Chem C* **2**, 6921-6939, doi:10.1039/c4tc00988f (2014).

10 Chen, L. & Liang, J. G. An overview of functional nanoparticles as novel emerging antiviral therapeutic agents. *Mat Sci Eng C-Mater* **112**, doi:ARTN 110924 10.1016/j.msec.2020.110924 (2020).

11 Du, T. *et al.* Carbon dots as inhibitors of virus by activation of type I interferon response. *Carbon* **110**, 278-285, doi:10.1016/j.carbon.2016.09.032 (2016).

12 Garg, P. *et al.* Exploring the role of triazole functionalized heteroatom co-doped carbon quantum dots against human coronaviruses. *Nano Today* **35**, 101001, doi:10.1016/j.nantod.2020.101001 (2020).

13 Jonjic, S. CMV immunology. *Cell Mol Immunol* **12**, 125-127, doi:10.1038/cmi.2014.132 (2015).

14 Gugliesi, F. *et al.* Where do we Stand after Decades of Studying Human Cytomegalovirus? *Microorganisms* **8**, doi:ARTN 685 10.3390/microorganisms8050685 (2020).

15 Griffiths, P. & Reeves, M. Pathogenesis of human cytomegalovirus in the immunocompromised host. *Nat Rev Microbiol* **19**, 759-773, doi:10.1038/s41579-021-00582-z (2021).

16 Kylat, R. I., Kelly, E. N. & Ford-Jones, E. L. Clinical findings and adverse outcome in neonates with symptomatic congenital cytomegalovirus (SCCMV) infection. *Eur J Pediatr* **165**, 773-778, doi:10.1007/s00431-006-0172-6 (2006).

17 Scarpini, S. *et al.* Development of a Vaccine against Human Cytomegalovirus: Advances, Barriers, and Implications for the Clinical Practice. *Vaccines (Basel)* **9**, doi:10.3390/vaccines9060551 (2021).

18 Erice, A. Resistance of human cytomegalovirus to antiviral drugs. *Clin Microbiol Rev* **12**, 286-297, doi:10.1128/CMR.12.2.286 (1999).

19 Guermouche, H. *et al.* Characterization of the dynamics of human cytomegalovirus resistance to antiviral drugs by ultra-deep sequencing. *Antiviral Res* **173**, 104647, doi:10.1016/j.antiviral.2019.104647 (2020).

20 Sadler, A., Williams, B. Interferon-inducible antiviral effectors. *Nat Rev Immunol* **8**, 559–568 (2008). https://doi.org/10.1038/nri2314

21 Tan, Y. S. & Lei, Y. L. Generation and Culture of Mouse Embryonic Fibroblasts. *Methods Mol Biol* **1960**, 85-91, doi:10.1007/978-1-4939-9167-9_7 (2019).

22 Vichai, V. & Kirtikara, K. Sulforhodamine B colorimetric assay for cytotoxicity screening. *Nat Protoc* **1**, 1112-1116, doi:10.1038/nprot.2006.179 (2006).

23 Crosse, K. M., Monson, E. A., Beard, M. R. & Helbig, K. J. Interferon-Stimulated Genes as Enhancers of Antiviral Innate Immune Signaling. *J Innate Immun* **10**, 85-93, doi:10.1159/000484258 (2018).

24 Wang, W. *et al.* Convergent Transcription of Interferon-stimulated Genes by TNF-alpha and IFN-alpha Augments Antiviral Activity against HCV and HEV. *Sci Rep* **6**, 25482, doi:10.1038/srep25482 (2016).

25 Aarreberg, L. D. *et al.* Interleukin-1beta Signaling in Dendritic Cells Induces Antiviral Interferon Responses. *mBio* **9**, doi:10.1128/mBio.00342-18 (2018).

26 Pulit-Penaloza, J. A., Scherbik, S. V. & Brinton, M. A. Type 1 IFN-independent activation of a subset of interferon stimulated genes in West Nile virus Eg101-infected mouse cells. *Virology* **425**, 82-94, doi:10.1016/j.virol.2012.01.006 (2012).

27 Dixit, E. *et al.* Peroxisomes are signaling platforms for antiviral innate immunity. *Cell* **141**, 668-681, doi:10.1016/j.cell.2010.04.018 (2010).

28 Du, T. *et al.* Glutathione-Capped Ag2S Nanoclusters Inhibit Coronavirus Proliferation through Blockage of Viral RNA Synthesis and Budding. *Acs Appl Mater Inter* **10**, 4369-4378, doi:10.1021/acsami.7b13811 (2018).

29 Barras, A. *et al.* High Efficiency of Functional Carbon Nanodots as Entry Inhibitors of Herpes Simplex Virus Type 1. *Acs Appl Mater Inter* **8**, 9004-9013, doi:10.1021/acsami.6b01681 (2016).